Magnetooptic Faraday effect in semiconductors

Yu. I. Ukhanov
Leningrad Polytechnic Institute
Usp. Fiz. Nauk 109, 667-694 (April 1973)

A review is given of the theoretical investigations of the rotation, in a magnetic field, of the plane of polarization of infrared electromagnetic waves traversing nonmagnetic semiconductors with cubic crystal lattices. It is shown that in the range of wavelengths corresponding to the interband or intraband optical absorption the Faraday effect can be used to determine the energy gaps, reduced effective masses, and the spectroscopic band-splitting factor. At longer wavelengths corresponding to the free-carrier absorption the Faraday effect can yield the average effective mass at the Fermi level and the Fermi energy can be found at low temperatures and in strong magnetic fields. Uniaxial deformation of crystals with many-valley bands makes it possible to use the free-carrier Faraday effect in the determination of the mass averaged out over an energy ellipsoid as well as the transverse component of the effective mass. A review is also given of the experimental results published for germanium, silicon, indium antimonide, gallium arsenide, and lead chalcogenides, which are optically isotropic in the absence of an external magnetic field.

CONTENTS

I. Introduction 236
II. Theory 236
III. Experimental Results 243
IV. Conclusions 248
Literature Cited 248

I. INTRODUCTION

The magnetooptic Faraday effect, which represents the rotation of the plane of polarization of an electromagnetic wave passing along a crystal in the direction of an external magnetic field, was first investigated for semiconductors by Kimmel in 1957[1] and since then it has been the subject of extensive theoretical and experimental studies aimed to obtain information on the energy band structure. An exceptionally large proportion of papers has been concerned with the analysis of the Faraday effect in the visible and infrared frequency range because in this range the effect is related unambiguously to the gaps between the critical points of the energy bands, to the effective carrier masses, and to other parameters of semiconductors.

The Faraday effect belongs to an extensive class of magnetooptic phenomena which arise in a crystal on the application of an external magnetic field and which can be arbitrarily divided into two groups. The first group is related to the splitting of the local energy levels of excitons, impurities, etc. This group includes the Zeeman effect (splitting of absorption lines and their polarization), the Voigt effect (birefringence near an absorption line), and the Maccaluso-Corbino effect (rotation of the plane of polarization near an absorption line). The most important member of this group, the Zeeman effect, is used widely in studies of the structure of local levels. The second group of the magnetooptic effects is associated with the appearance of the Landau sub-bands in the conduction and valence bands. Optical transitions between the Landau sub-bands in different bands give rise to the interband effects, the most important of which is manifested by oscillations of the fundamental absorption. The other effects, such as the rotation of the plane of polarization (Faraday effect), birefringence (Voigt effect), oscillations of the reflection coefficient, etc., are consequences of the oscillations in the fundamental absorption. Electron transitions between the Landau sub-bands within the same (conduction or valence) band give rise to the intraband Faraday and Voigt effects, plasma reflection, cyclotron resonance, etc.

Magnetooptic methods for investigating the energy band structure of crystals,[2] oscillations of the fundamental absorption in germanium,[3] and the combination resonance[4] have all been considered in the present journal. Reviews on the Faraday effect have been published in foreign journals[5-7] but in the period between the appearance of the latest of these reviews[7] a basically new approach has been developed to the application of the Faraday effect in studies of the band structure of semiconductors. Therefore, it has seemed desirable to review the Faraday effect again, including the latest investigations.

The total number of papers published on the Faraday effect is very large and the present review is concerned only with the rotation of the plane of polarization of infrared radiation in nonmagnetic semiconducting materials with cubic crystal lattices. Experimental results are reviewed for semiconducting materials belonging to group IV (germanium and silicon), III-V compounds (indium antimonide and gallium arsenide), and IV-VI compounds (lead chalcogenides), which are optically isotropic in the absence of an external magnetic field. The bibliography at the end of the review consists mainly of papers published after 1965 and not included in[8].

II. THEORY

1. Influence of a Magnetic Field on the Spectrum of Energy Levels in Bands

The application of an external magnetic field (an induction B) to a cubic crystal with the quadratic dispersion law induces an optical anisotropy and makes the dispersion more complex. The carrier energy becomes

 Copyright © 1974 American Institute of Physics

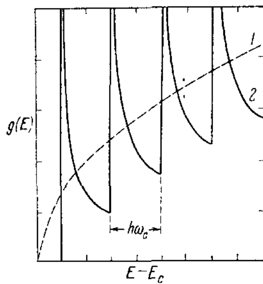

FIG. 1. Energy spectrum of the density of states in a simple band in the absence of an external magnetic field (1) and in the presence of such a field (2).

FIG. 2. Landau levels in the conduction band and in three branches of the valence band of germanium. The arrows identify the transitions corresponding to the π spectrum ($\Delta l = 0, -2, \Delta M = 0$).

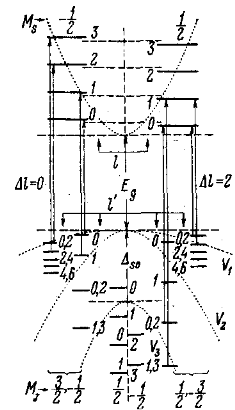

quantized in a plane perpendicular to **B** but the levels remain quasicontinuous along **B** forming series of one-dimensional Landau sub-bands. The density of states in the simplest possible nondegenerate band (derived for the quadratic dispersion law and **B** = 0) can be represented by the following formula[9]

$$g(E) = (2\pi)^{-2}(2m_d/\hbar^2)^{3/2} \sum_{l=0}^{l_{max}} \hbar\omega_c [E - E_c - (l+1/2)\hbar\omega_c \pm (1/2)\beta g B]^{-1/2}; \quad (1)$$

here, $\hbar$ is the Planck constant divided by 2π, m_d is density-of-states effective mass, ω_c is the cyclotron frequency, $\omega_c = Be/m_c$, m_c is the conductivity effective mass, E_c and E are the energies of the band edge and of a carrier in a band, l is a positive integer for which the denominator is positive, g is the spectroscopic splitting factor, and β is the Bohr magneton. This dependence is represented in Fig. 1 (without allowance for spin) by the continuous curve. The dashed curve represents the density of states g(E) for **B** = 0. The energies corresponding to the infinitely high density of states (Landau levels) are separated by intervals $h\omega_c$ proportional to the magnetic induction and inversely proportional to the effective mass. The band edge shifts by an amount $h\omega_c/2$, which corresponds to an increase in the width of the forbidden band in a magnetic field by an amount $h(\omega_{c,n} + \omega_{c,p})/2$ where $\omega_{c,n}$ and $\omega_{c,p}$ are the cyclotron frequencies for the conduction and valence bands, respectively.

If a band is of the multiplet type, the Landau levels are formed in each band (branch) and the energy gaps between them are $h\omega_c$ only for large values of l, whereas levels corresponding to small values of l are nonequidistant. A review of the work done on this subject can be found in the paper of Zakharchenya and Seĭsyan.[3] Recently, Lee and Fan[10] calculated the Landau levels for all the branches (bands) of germanium in a strong magnetic field.

Figure 2 shows the spectrum of the Landau levels in the conduction and valence bands of germanium for $k_z = 0$. The Landau levels in the valence band of InSb are basically similar to those encountered in germanium but they differ in details. The differences are due to the absence of an inversion center in the zinc-blende lattice of InSb, because of which the branches V_1 and V_2 are degenerate only at the point **k** = 0 and the maxima of the branch V_1 are shifted relative to **k** = 0 (the maximum of the branch V_2 is located at this point) in the [111] direction and are located above the maximum of the branch V_2. The effective mass in the conduction band and the corresponding factor g_c depend strongly on the magnetic field and the Landau levels are not equidistant because of a considerable departure from the quadratic dispersion law. In weak fields the spin splitting of the levels near the edge of the conduction band exceeds one-third of $h\omega_{c,n}$ because the g_c factor of the conduction band reaches −48.

In the case of PbTe the valence and conduction bands are nondegenerate (if spin is ignored) and their absolute extrema are located at the point L in the Brillouin zone. The dispersion law for these bands is not quadratic but it is basically similar to the dispersion law of the conduction band of InSb. Therefore, in calculations of the Landau levels in the conduction and valence bands of these compounds, which have ellipsoidal constant-energy surfaces, the effective mass which occurs in the expression for the cyclotron frequency is assumed to be[11]

$$m_c = m_t\,[K/(K\cos^2\varphi + \sin^2\varphi)]^{1/2},$$

where $K = m_l/m_t$, m_l and m_t are the longitudinal and transverse components of the mass ellipsoid, and φ is the angle between the axis of rotation of the ellipsoid and the direction of **B**. In this case the spectroscopic splitting factor is

$$g = \pm (g_l^2\cos^2\varphi + g_t^2\sin^2\varphi)^{1/2},$$

where g_l and g_t are the components of the g factor parallel and perpendicular to the ellipsoid axis: $g_l = \pm 2m_0/m_t$, $g_t = 2$.

The energy level scheme becomes much more complex if allowance is made for the Coulomb interaction between bound electron-hole pairs.[3] Under certain conditions (sufficiently wide forbidden band E_g, relatively low static or low-frequency permittivity, and low impurity concentration) the exciton energy states form a hydrogenic spectrum below the bottom of the conduction band. An external magnetic field produces a similar spectrum below each Landau level in the conduction band and the energy of the ground state decreases with increasing serial number of the level and increases with increasing magnetic field.

In the absence of an external magnetic field and at low temperatures the free carriers (density N, degenerate at T = 0°K) occupy levels near the edge of the conduction or valence band of an extrinsic semiconductor. The occupied levels extend right up to the Fermi level $E_F^{(0)}$, whose energy is related in an unambiguous manner to the carrier density and the band parameters. In the case of a crystal subjected to an external magnetic field the relationship between the carrier density N and the Fermi energy E_F becomes more complex. For a standard spin-degenerate band this relationship can be represented by the formula[9]

$$N = 2\sqrt{2}\,\hbar^{-2}\omega_c m_{n,p}^{3/2} \sum_l [E_F - (l+1/2)\hbar\omega_c]^{1/2}. \quad (2)$$

It follows from this formula that the Fermi energy oscillates with increasing magnetic field and falls rela-

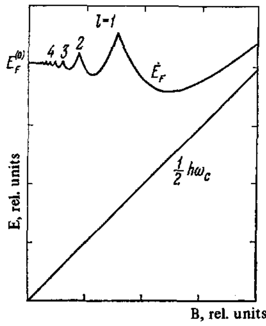

FIG. 3. Dependences of the energies of the Fermi and zeroth Landau levels on the magnetic induction under conditions of strong degeneracy.

tive to the zeroth Landau level. The magnetic-field dependences of the energies of the Fermi level and of the zeroth Landau level are plotted in Fig. 3 for the strongly degenerate case. We can see that the Fermi energy oscillates with rising magnetic field and the oscillation maxima correspond to magnetic fields in which the Landau level crosses the Fermi level so that the free carriers leave the corresponding Landau subband.

It is worth noting the slow asymptotic approach of the Fermi level to the zeroth Landau level in strong magnetic fields. This occurs because the zeroth Landau level is the lowest one in a band and, therefore, it cannot be emptied until the magnetic induction reaches infinity.

These oscillations of the Fermi energy in an external magnetic field are the cause of the oscillations of the magnetic susceptibility (de Haas—van Alphen effect), electrical conductivity (Shubnikov—de Haas effect), and rotation of the plane of polarization (Faraday effect) in the frequency range $\omega \lesssim \omega_g$.

2. Interband Effect

The changes in the energy bands induced by an external magnetic field alter the dispersion relationship for the complex refractive index of a crystal. If the conduction band is empty, the valence band is filled, B is directed along the z axis, light is traveling along the x axis, and the electric field of the incident light wave is parallel to the z axis (π spectrum) the dispersion law is[12]

$$\begin{gathered}(n-ik)^2=1+(8\pi e^2/m_0^2\hbar)\sum_{\xi}|P^{x}_{c,v}(\xi)|^2[\omega_{ll'}(\omega_{ll'}^2-\omega^2+i\omega\omega')]^{-1},\\ \omega_{ll'}=\omega_g+(h^2k_z^2/2m_*)+(l+1/2)\omega_{c,n}+(l'+1/2)\omega_{c,p}+\mu\beta B,\\ \mu=M_lg_l-M_{l'}g_{l'},\ m_*=m_nm_p/(m_n+m_p);\end{gathered}\tag{3}$$

here, n is the real refractive index, k is the extinction coefficient, M_l and $M_{l'}$ are spin quantum numbers equal to $\pm 1/2$, g_l and $g_{l'}$ are the spectroscopic factors of the conduction and valence bands, $\tau = 1/\omega'$ is the phenomenological relaxation time introduced to take account of the finite level lifetime, $P^{x}_{c,v}(\xi)$ is the matrix element of the momentum in the effective mass approximation, $\xi = k_x$ or k_z, l and l' are the quantum numbers of an electron in a magnetic field. Formula (3) contains additional angular coefficients for other orientations of the electric vector of the light wave and of its propagation vector relative to B.

The interband electron transitions are subject to the selection rules applicable to the quantum numbers l and M: $\Delta l = l - l' = 0$, $\Delta M = 0, \pm 1$, which are governed by the symmetry of the wave functions of the band edges and by the orthogonality of the spin wave functions. The selection rule $\Delta l = 0$ means that the first-order optical transitions are allowed if an electron is transferred by a photon from a magnetic Landau level l' in the valence band to a Landau level in the conduction band which has the same number $l = l'$. The selection rule for the spin quantum number $\Delta M = 0, \pm 1$ imposes restrictions on the polarization of light. If $\Delta M = 0$, the first-order transitions, identified by arrows in Fig. 2, are allowed for light whose electric vector is $\mathbf{E} \parallel \mathbf{B}$ and propagation vector is $\mathbf{\Gamma} \parallel \mathbf{B}$. This case is analogous to the π spectrum in the atomic Zeeman effect. For $\Delta M = \pm 1$, we must have $\mathbf{E} \perp \mathbf{B}$ and $\mathbf{\Gamma} \perp \mathbf{B}$ (σ spectrum). If light travels parallel to the magnetic field (Faraday orientation), the transitions are allowed only for circularly polarized light: $\Delta M = +1$ for the left-handed circular polarization and $\Delta M = -1$ for the right-handed polarization (σ_+ and σ_- spectra). The selection rules for the higher-order transitions are different.[3]

Formula (3) and the selection rules can be used to calculate the frequency dependences of the refractive index and the extinction coefficient for natural (unpolarized) and for linearly or circularly polarized light. These dependences can then be used to find the spectra of all the magnetooptic effects.

The rotation of the plane of polarization of light passing across a crystal of thickness d in a magnetic field parallel to the propagation vector of light is calculated using the nondiagonal elements σ_{xy} of the electrical conductivity tensor or the difference between the refractive indices n_- and n_+ for the right- and left-hand circularly polarized waves:

$$\theta=(d/2cn)\,\sigma_{xy}=(\omega d/2c)\,(n_--n_+).\tag{4}$$

The difference between the absorption coefficients α_- and α_+ means that the ellipticity of the Faraday effect is $\eta = \tanh(\alpha_- - \alpha_+)/d$.

In the absence of an external magnetic field the refractive index has a maximum in the region of ω_g. In strong fields B the maxima predicted by Eq. (3) correspond to the Landau levels if the contributions of excitons are ignored. Thus, the interband Faraday effect may be considered in two extreme cases: 1) weak fields and $\omega < \omega_g$; 2) strong fields and $\omega > \omega_g$.

In the first case, the theory of Boswarva, Howard, and Lidiard[13,14] predicts the following frequency dependence of the rotation in a pure crystal:

$$\begin{gathered}\theta_{\omega<\omega_g}=\theta_*f(x),\\ \theta_*=\sqrt{2}\,e^2m_*^{3/2}|P^{x}_{c,v}(\xi)|^2\gamma Bd\,(m_0^2\hbar^{5/2}\omega_g^{3/2}nc)^{-1},\\ f(x)=f(\omega/\omega_g)=(1/x)[(1-x)^{-1/2}-(1+x)^{-1/2}]-1,\\ \gamma=(g_c+g_v)\beta/2.\end{gathered}\tag{5}$$

A more cumbersome expression has been obtained by Roth,[15] who took account of the complex structure of the valence band. In the frequency range $\omega < \omega_g$ both theories predict $f(x) \propto \omega^2$, i.e., the frequency dependence of the rotation of the plane of polarization is similar to the classical dependence deduced for an elementary oscillator.[14] It is evident from Eq. (5) that the sign of the rotation is governed by the relationship between g_c and g_v and their signs.

In a degenerate semiconductor the angle of rotation θ in the range $\omega < \omega_g$ depends strongly on the impurity concentration, carrier density, and temperature because of a paramagnetic contribution resulting from the interaction between localized centers and the external magnetic field[16-21] Calculations carried out for simple

bands with the Fermi distribution of carriers yield the following expression for the dispersion of the angle of rotation in the case of low fields and weak absorption:

$$n(\omega)\,\theta(\omega)=\frac{2\pi d}{c}\,\frac{M\hbar e^2\,|P^x_{c,v}(\xi)|^2}{m_0^2 V}\sum_{n,E}\left\{\frac{F^\alpha_+-F^\beta_-}{E^2-(h\omega)^2}-\frac{2(g_c-g_v)\beta BE(F^{(0)}-1)}{[E^2-(h\omega)^2]^2}\right\}, \tag{6}$$

where the summation is carried out over all the energy levels:

$$E=E_g^\pm=E_g+(l+1/2)\,h(\omega_c+\omega_v)+(\hbar^2k_z^2/2)(m_c^{-1}+m_v^{-1})\pm(1/2)(g_c-g_v)\beta B.$$

The Fermi function $F_\pm$ depends on the variable $(E - E_g - E'_{F\pm})/kT'$ where

$$E'_{F\pm}=[1+(m_c/m_v)]E_F^{(0)}\pm(1/2)[g_v+(m_c/m_v)g_c]\beta B,$$

$T' = 1 + (m_c/m_v)T$ and $E_F^{(0)}$ is the Fermi energy measured from the bottom of the conduction band in the absence of the magnetic field. The first term in Eq. (6) represents solely the contribution of the region in the vicinity of the Burstein-Moss energy $E'_g = E_g + [1 + (m_c/m_v)]F_F^{(0)}$. The second term (which will be referred to as II) describes the usual interband rotational reduced by "blocking" of the Landau levels.

The oscillatory terms in the angle of rotation, which are of the same origin as the oscillations of the magnetoresistance in the Shubnikov-de Haas effect or the oscillations of the magnetic susceptibility in the de Haas-van Alphen effect, are contained in the first term in Eq. (6), which can be represented in the form which makes clear the physical origin of these oscillations:

$$n(\omega)\,\theta(\omega)=\frac{2\pi d}{c}\,\frac{M\hbar e^2\,|P^x_{c,v}(\xi)|^2}{m_0^2[(E'_g)^2-(h\omega)^2]}\,\frac{N_\alpha-N_\beta}{V}+\mathrm{II}. \tag{7}$$

Thus, the effects considered here depend directly on the difference between the populations of two Kramers states of the Landau sub-bands. This difference is a complex function of the free-carrier density in a given band and of the magnetic field. Equation (7) can be expanded to

$$n(\omega)\,\theta(\omega)=\frac{2\sqrt{2}\,M^*d}{\pi c}\,\frac{e^2\mu_{c,v}^{3/2}\,|P^x_{c,v}(\xi)|^2}{h^2m_0^2[(E'_g)^2-(h\omega)^2]}\times\left\{(E_F^{0\prime})^{1/2}\left(g_v+\frac{m_c}{m_v}g_c\right)\beta B+\frac{\pi(\beta B)^{1/2}m_ckT}{m_0\mu_{c,v}^{3/2}}\sum_{r=1}^{\infty}\frac{(-1)^{r+1}}{r^{1/2}}\times\frac{\sin[r\pi(g_v+(m_c/m_v)g_c)\mu_{c,v}]\sin[(2\pi rE_F^0/\hbar\omega_c)+(\pi/4)]}{\mathrm{sh}[2\pi^2rkT/h\omega_c]}\right\}+\mathrm{II}, \tag{8}$$

where $\mu_{c,v}^{-1} = (m_0/m_c) + (m_0/m_v)$, M^* is the number of equivalent valleys in the band under consideration ($M^* = 4$ for the conduction band of germanium and of lead chalcogenides). Here, the effective mass and the g factors are found by summing over all the band levels.

An analysis of Eq. (8) shows that the total angle of rotation is governed by the competition between two large contributions associated with the absorption of the right- and left-hand polarized waves. The greatest contribution is made by the low-lying Landau levels. In the simplest case of a semiconductor with standard nondegenerate (spin is ignored) bands a right-handed (left-handed) polarized wave causes electron transitions from the valence-band levels with spins directed upward (downward) to the conduction-band levels with spins oriented downward (upward). Consequently, all the interband transitions to the conduction-band levels with the same spin states make contributions which are of the same sign. This contribution is positive for the levels with spin $-1/2$, i.e., for the downward-oriented spin, and negative for the levels with spin $+1/2$, i.e., for the upward-oriented spin.

The total rotation associated with the magnetic levels in the conduction band is governed by the matrix elements, which relate the initial and final states, and by the density of the final empty states. In the first approximation, the matrix element is independent of the wave vector k_z, whereas the density of the Landau levels has sharp peaks at $k = 0$. Thus, the rotation of the plane of polarization associated with any Landau level is governed by a narrow region in the k space near $k = 0$.

A change in the population of the lowest Landau levels alters the balance of the contributions to the components n_+ and n_- in Eq. (4) and this gives rise to oscillations of the rotation of the plane of polarization. At a fixed electron density in the conduction band the population of the Landau sub-bands varies continuously with increasing magnetic field and this gives rise to an oscillatory unbalance of the components n_+ and n_-.

In the quantum limit, when the Fermi level E_F is of the order of several $h\omega_c$ units and the thermal energy of electrons kT is less than the splitting of the Landau levels with different spin orientations, i.e., $kT < g\beta B$, the maxima of the oscillations of the angle of rotation correspond to magnetic fields in which the Landau sublevels with spin-up and spin-down orientations rise alternately above the Fermi level making possible interband transitions which make contributions of different signs to the total angle of rotation.

Dennis, Smith, and Summers[22] calculated these contributions for different Landau sublevels in the conduction band of indium antimonide making allowance for the complex structure of the valence band and for the conduction-band nonparabolicity. The relative contributions to the total angle of rotation are listed in Table I for $B = 3.0$ T and $\omega = \omega_g/2$, where ω_g is the frequency corresponding to the forbidden band width. It is evident from Table I that the relative amplitude of the oscillations increases with decreasing Landau quantum number; moreover, the absolute contribution of a spin-up level is greater than of a spin-down level.

Extremal values of the angle of rotation generally correspond to magnetic fields given by the equation

$$E_F=(l+1/2)\,h\omega_c\pm(1/2)\,\hbar\omega_s,$$

which can be rewritten in the form

$$l=E_Fm_c/heB-(1/2)[1\pm(\omega_s/\omega_c)]; \tag{9}$$

here, $\omega_s = g\beta B$ and E_F is given by Eq. (2).

TABLE I. Calculated contributions to total angle of rotation for $h\omega = E_g/2$ and n-type InSb ($B = 3.0$ T)

Level in conduction band	Relative contribution to total interband rotation
0↓	Very large and negative
1↑	+3.8
1↓	−3.28
2↑	+1.8
2↓	−1.75
3↑	+1.1

Thus, the Landau quantum numbers corresponding to extrema of the angle of rotation are proportional to the reciprocal of the magnetic induction. The straight lines represented by Eq. (9) have the slope $E_F m_c/e\hbar$ and intersect the 1/B axis at the points $1/B_- = [1 - (\omega_s/\omega_c)]e\hbar/2m_cE_F$ and $1/B_+ = [1 + (\omega_s/\omega_c)]e\hbar/2m_cE_F$, which are separated by $(1/B_-) - (1/B_+) = \hbar gB/E_F$. The two parameters $E_F m_c/e\hbar$ and $\hbar gB/E_F$ include three unknowns E_F, m_c, and g, so that if we know one of them we can calculate the other two. A comparison of Eqs. (5) and (9) shows that experimental investigations of the interband Faraday effect in the $\omega < \omega_g$ frequency range can yield additional information on the energy band parameters of a semiconductor with a degenerate free-carrier gas at very low temperatures.

In the frequency range $\omega > \omega_g$ and for the simplest possible nondegenerate bands (ignoring the Coulomb interaction between carriers) the angle of rotation is given by[12]

$$\theta(\omega) \propto \sum_{l=0}^{l_{max}} (F_l^+ - F_l^-),$$

$$F_l^{\pm} = \frac{\omega_g^{5/2}}{\omega^2}\left[\frac{\{[(\omega_l^{\pm}-\omega)^2+(\omega')^2]^{1/2}+(\omega_l^{\pm}-\omega)\}^{1/2}}{\sqrt{2}[(\omega_l^{\pm}-\omega)^2+(\omega')^2]^{1/2}} + (\omega_l^{\pm}+\omega)^{-1/2} - 2(\omega_l^{\pm})^{-1/2}\right],$$

$$\omega_l^{\pm} = \omega_g + (l+1/2)\omega_* \pm (1/2)(g_c+g_v)\beta' B,$$

$$\omega_* = \omega_{cn} + \omega_{cp}, \quad \beta' = \beta/h; \qquad (10)$$

here, the summation is carried out up to the Landau number l_{max}, beginning from the values of $F_l^{\pm}$ which are practically independent of the frequency. It is evident from Eq. (10) that the angle of rotation oscillates reaching its maxima at the points $\omega = \omega_l^+$ (l = 0, 1, 2, ...) and its minima at the points $\omega = \omega_l^-$. The distance between the maxima of the angle of rotation is ω^* and that between the maxima and minima is $(g_c + g_v)\beta' B$. The oscillation waveform in Eq. (10) is governed by $\omega' = \tau^{-1}$. The best agreement between the calculated and experimental oscillatory dependences of the angle of rotation is obtained if allowance is made for the predominant carrier-scattering mechanism (acoustic or optical phonons, impurities, etc.).[23]

An even better description of the line profiles in the rotation spectrum and of the dependence of the line energy on the magnetic field is obtained if allowance is made for the Coulomb interaction between carriers. In this case the rotation is associated with optical transitions from the valence band not to the Landau levels in the conduction band but to exciton levels located below the Landau levels.[24,25] This allowance should be made not only at low temperatures but also at room temperature when the exciton peaks are usually absent from the absorption spectra recorded in zero magnetic field.[25]

The spectrum of the angle of rotation of germanium was calculated by Suzuki and Hanamura[25] making allowance for the presence of excitons:

$$\theta_{ex}(\omega) = \frac{\pi e^2 d}{2nc\hbar\omega_g} \sum_{M_cM_vl} [|(v_-)_{M_cM_v}|^2 - |(v_+)_{M_cM_v}|^2] \,\mathrm{Re}\, \frac{|U_{M_cM_vl}(0)|^2}{\omega_{l_0} - \omega + i\tau_l^{-1}},$$

where

$$(v_{\pm})_{M_cM_v} = \Omega^{-1} \int \Phi_{M_c}^* (v_x \pm iv_y) \Phi_{M_v} d\tau,$$

v is the velocity operator, $\Phi = \Phi_{M_c}$ ($M_c = \pm 1/2$) and Φ_{M_v} (M_v = −3/2, −1/2, 1/2, 3/2) are the Bloch functions for the conduction and valence bands at k = 0, U_l is the eigenfunction of the l-th quantum state of the motion of an electron-hole pair, τ_l is the relaxation time, and $\hbar\omega_{l_0} = E - E_0$. The summation is carried out over all the quantum states in the conduction and valence bands. The dependence $\theta_{ex}(\omega)$ calculated in this way for 300°K and B = 88 kG = 8.8 T is plotted in Fig. 4. For the sake of comparison the same figure includes also the spectrum $\theta(\omega)$ calculated in[12] but without allowance for the exciton contribution, which can be seen to be quite different from $\theta_{ex}(\omega)$, particularly in the region of the first band (Fig. 4).

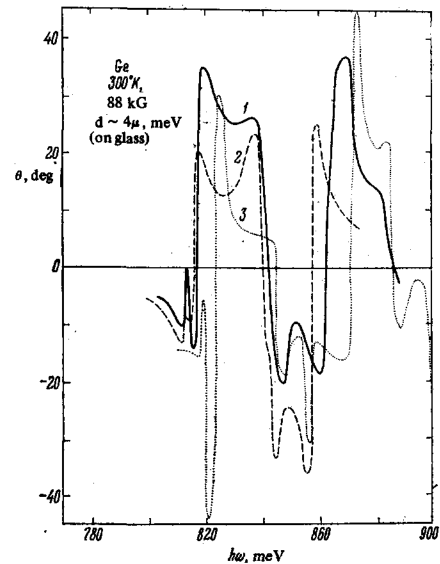

FIG. 4. Oscillatory spectra of the interband Faraday effect in germanium: 1—experimental results; [41] 2—theory allowing for excitons; [25] 3—theory not allowing for excitons. [26]

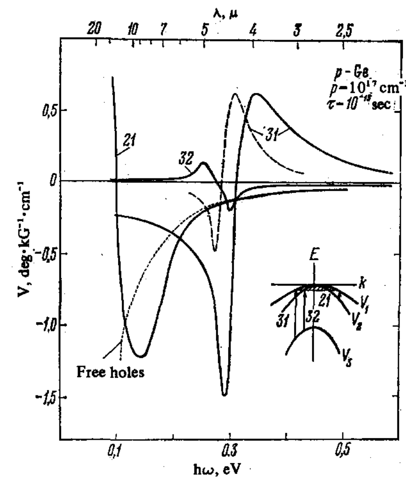

FIG. 5. Theoretical spectra of the intraband effect in p-type Ge. The continuous and dotted curves are the calculations reported in [10], the dashed curve is taken from. [28] The numbers identify the transitions between the branches 3, 2, and 1 of the valence band, shown in the lower right-hand corner of the figure.

Dependences similar to Eqs. (5) and (10) have been derived in[12,25,27] for the interband Voigt, Kerr, and other effects (for $\omega < \omega_g$ and $\omega > \omega_g$) which are quadratic in the magnetic field but sufficiently strong to be experimentally detectable in reasonably high magnetic fields. Allowance for the damping by introduction of the relaxation time makes it possible to calculate approximately[27] the form of oscillations of the Voigt effect $\delta(\omega)$, determine the g factors of the conduction

and valence bands, and calculate the relaxation times from the ratio $\delta_{max}/\theta_{max} \approx \gamma\beta\tau$, where δ_{max} and θ_{max} are the maximum values of the phase shift and of the angle of rotation.

3. Intraband Effect

If an energy band consists of several branches, optical transitions can take place between these branches, as shown in the lower right-hand corner in Fig. 5 for the valence band of germanium. Consequently, the magnetooptic effects take place between the band branches. The spectra of the Faraday effect associated with such intraband transitions are calculated for germanium in[10,28] and are plotted in Fig. 5 for a hole density of 10^{17} cm^{-3} and $\tau = 10^{-13}$ sec. Lee and Fan[10] made an allowance for changes in the complex structure of the valence band in strong magnetic fields and, therefore, their calculations (continuous and dotted in Fig. 5) are more correct than the calculations of Walton and Mishra[28] (dashed curve). It is evident from Fig. 5 that the 3–5 μ region is dominated by the contribution of the $V_3 \rightarrow V_1$ transitions whereas in the 6–15 μ region the rotation is due to the free holes (θ_1) and the $V_2 \rightarrow V_1$ transitions (θ_2); in the 5–8 μ range the dependences $\theta_1(\omega)$ and $\theta_2(\omega)$ are almost identical but at $\lambda > 13\ \mu$ the component $\theta_1(\omega)$ predominates.

The intraband rotation spectra have not yet been calculated for other semiconductors.

4. Free-Carrier Effect

In the energy range $\hbar\omega < E_g$ ($\omega_{L_0} < \omega < \omega_g$) the magnetooptic effects in the degenerate semiconductors appear because of the interaction between photons and free carriers. The problem can be solved in sufficient detail with the aid of the Boltzmann transport equation. In the simplest approximation of an isotropic effective carrier mass $m_{n,p}$ and a relaxation time $\tau_{n,p}$ we obtain[8] the following expression for the conductivity tensor:

$$\sigma = \begin{vmatrix} \sigma_{xx} & \sigma_{xy} & 0 \\ \sigma_{yx} & \sigma_{yy} & 0 \\ 0 & 0 & \sigma_{zz} \end{vmatrix}, \tag{11}$$

where

$$\sigma_{xx} = \sigma_{yy} = \omega_p^2 \varepsilon_\infty \varepsilon_0 (\tau_{n,p}^{-1} + i\omega)[(\tau_{n,p}^{-1} + i\omega)^2 + \omega_c^2]^{-1},$$
$$\sigma_{xy} = -\sigma_{yx} = \omega_c \omega_p^2 \varepsilon_\infty \varepsilon_0 [(\tau_{n,p}^{-1} + i\omega)^2 + \omega_c^2]^{-1},$$
$$\sigma_{zz} = \omega_p^2 \varepsilon_\infty \varepsilon_0 (\tau_{n,p}^{-1} + i\omega)^{-1}, \quad \omega_c = Bem_{n,p}^{-1}, \quad \omega_p^2 = e^2 N_{n,p} (\varepsilon_\infty \varepsilon_0 m_{n,p})^{-1},$$

$N_{n,p}$ are the densities of electrons or holes, ϵ_∞ is the high-frequency permittivity, and ϵ_0 is the permittivity of vacuum in SI units.

The optical constants associated with the conductivity (11) depend on the magnetic field orientation, the direction of propagation of light, and the electric vector of the light wave. We can isolate two special cases which we shall call longitudinal and transverse: they correspond to the propagation vector parallel and perpendicular to the induction of the external magnetic field.

In the longitudinal case (Faraday orientation) a linearly polarized light wave can be represented by left- and right-hand circularly polarized component for which the effective conductivity is

$$\sigma_\pm = \sigma_{xx} \pm i\sigma_{xy} = \omega_p^2 \varepsilon_\infty \varepsilon_0 [\tau_{n,p}^{-1} + i(\omega \mp \omega_c)]^{-1}, \tag{12}$$

where the plus sign corresponds to a left-handed polarized wave and the minus sign to a right-handed wave. It is clear from Eq. (12) that as $\omega \rightarrow \omega_c$ the electrical conductivity $\sigma_\pm$ exhibits two singularities corresponding to the resonance absorption of energy, which increase in amplitude with the degree to which the condition $\omega_c \tau_{n,p} \gg 1$ is satisfied.

Let us now consider Eq. (9) and assume that the following conditions, which can be realized in practice, are satisfied: $\omega > \omega_p > \omega_c$ (weak magnetic fields), $\omega_c \tau_{n,p} \gg 1$ (infrared range of wavelengths, where $\omega > \omega_{L_0}$, i.e., the working frequency is higher than the frequency of one-phonon resonance), and $n^2 \gg k^2$ (weak absorption). In this situation we obtain the formula

$$n_\pm^2 \approx \varepsilon_\infty \{1 - [\omega_p^2/\omega(\omega \mp \omega_c)]\}, \tag{13}$$

which reduces to the following form for $B = 0$:

$$n^2 \approx \varepsilon_\infty [1 - (\omega_p^2/\omega^2)].$$

The above form is used widely[8] in determination of the effective mass of free carriers from the reflection spectra in the absence of a magnetic field.

Subject to the conditions $n^2 \gg k^2$ and $\omega > \omega_p > \omega_c$, Eqs. (4) and (13) yield the following formula for the angle of rotation of the plane of polarization in the free-carrier case:

$$n(\omega)\theta(\omega) = (\varepsilon_\infty d/2c)\omega_p^2 \omega_c/\omega^2 = e^3 B N_{n,p} d/2c\varepsilon_0 \omega^2 m_f^2, \tag{14}$$

which shows that the rotation is proportional to the carrier density $N_{n,p}$ and inversely proportional to the square of the effective mass m_f. Therefore, the value of m_f can be determined from the dependence $n\theta(\lambda^2)$ without analyzing the scattering mechanisms provided the carrier density is independent of these mechanisms (this is true, for example, of a degenerate free-carrier gas). Since Eq. (14) includes the square of the effective mass m_f, the error in the determination of this mass should be less than in the calculation from the reflection spectra (other conditions being equal).

An analysis of Eq. (14) for different types of energy bands shows[6,7,11,28,29] that the value of m_f generally differs from the conductivity effective mass m_R deduced from the dispersion of the refractive index, i.e., from plasma or magnetoplasma reflection or from cyclotron resonance. This difference is due to the structure of the band containing free carriers. We shall now consider several special cases.

1) A simple band consisting of one branch $E(\mathbf{k})$ with the quadratic dispersion law and with spherical constant-energy surfaces. In this case $m_f = m_R$.

2) A band has one branch $E(k)$ with a nonquadratic dispersion law and constant-energy surfaces are spherical. In this case

$$m_f = m_R = h^{-2}(\partial E/k\,\partial k)_F^{-1}. \tag{15}$$

Here, F denotes that the wave vector k_F corresponds to the Fermi level.

3) Two simple "spherical" bands degenerate at $k = 0$ with masses m_1 and m_2, where $m_1 \neq m_2$. Using the relationship $(m_1/m_2)^{3/2} = N_1/N_2$ and assuming that $N = N_1 + N_2$, we find that $m_f = m_R(m_1 m_2)^{1/2}$, where $m_R = (m_1^{3/2} + m_2^{3/2})/(m_1^{1/2} + m_2^{1/2})$. Consequently,

$$(m_R/m_f)^2 = \alpha^{1/2}(1 + \alpha^{1/2})/(1 + \alpha^{3/2}), \tag{16}$$

where $\alpha = m_2/m_1$. An analysis of Eq. (16) shows that $m_R > m_f$ if $\alpha \neq 1$. Using $N/m_R = (N_1/m_1) + (N_2/m_2)$

and $N/m_f^2 = (N_1/m_1^2) + (N_2/m_2^2)$ we find that $m_R \approx m_1(1+\alpha^{-1/2})^{-1}$ and $m_f^2 \approx m_1^2(1+\alpha^{1/2})^{-1}$ so that

$$m_f^2 + m_R m_1 - m_1^2 \approx 0. \quad (17)$$

Thus, having determined m_R from the reflection spectra and m_f from the Faraday effect, we can use Eqs. (16) and (17) to estimate the masses of light and heavy holes in a band.

4) Constant-energy surfaces in the form of ellipsoids of revolution and the quadratic dispersion law. In this case $m_f^2 = m_t^2 3K/(2+K)$ and $m_R = m_t 3K/(2K+1)$. Consequently,

$$m_f^2/m_R = m_t(2K+1)/(K+2) \quad (18)$$

and

$$(m_R/m_f)^2 = 3K(K+2)/(2K+1)^2, \quad (19)$$

i.e., m_f is greater than m_R for any value of $K = m/m_t \neq 1$. We note that the right-hand side of Eq. (19) is the anisotropy factor in the Hall coefficient. It is worth noting that in case 3 the value of m_f is smaller than m_R, whereas in case 4 the value of m_f is greater than m_R.

Gurevich and Ipatova[30] demonstrated that in many-valley semiconductors the angle of rotation is anisotropic in a strong magnetic field and, therefore, the components of the mass ellipsoid m_l and m_t can be determined from the Faraday effect.

5) Ellipsoidal constant-energy surfaces obeying the Kane dispersion law.[11] In this case, we have

$$(m_R/m_f)^2 = [3K(K+2)/(2K+1)^2]\, {}^0\mathcal{L}_{-2}^{3/2}\, {}^0\mathcal{L}_0^{3/2}/({}^0\mathcal{L}_{-1}^{3/2})^2$$

and if the degeneracy is strong, the above expression is identical with Eq. (19) to within 1–2% because in this case the ratio of the integrals $\mathcal{L}$ is close to unity.

Uniaxial compression reduces the lattice symmetry of crystals with diamond, zinc-blende, and rocksalt structures, i.e., the compressed crystal becomes uniaxial instead of cubic. An external load of this kind lifts the degeneracy of the equivalent valleys in the conduction or valence band (the latter applies to lead chalcogenides). Consequently, the free-carrier Faraday effect becomes anisotropic and we can determine the components m_l and m_t. Birefringence can be eliminated by investigating the Faraday effect under a load directed parallel to the magnetic field and to the light propagation vector. Moreover, the crystal itself should be oriented in a suitable manner relative to the direction of the load.

In the case of silicon the six equivalent conduction-band ellipsoids are elongated along the fourfold axes [100], [010], and [001]. Therefore, compression along the [100] axis results in a descent of two equivalent valleys corresponding to the directions [100] and [$\bar{1}$00] and an ascent of the other four valleys. If the magnetic field, the load, and the light propagation vector are parallel to the [100] axis, the Faraday effect yields the transverse component of the effective mass m_t.

A similar situation occurs in n-type germanium and in n- and p-type lead chalcogenides if the magnetic field, the load, and the direction of propagation of light are parallel to the threefold axis [111] because the constant-energy surfaces of the conduction band of germanium and of both bands of lead chalcogenides are ellipsoids of revolution elongated along the [111] axis.

If $\omega \gg \omega_l, \omega_t, \omega\tau \gg 1$, and $k_\pm \ll n_\pm$, the angle of rotation of the plane of polarization for a six-ellipsoid semiconductor is given by[31]

$$\theta_{s(6)} = (e^3B\lambda^2 d/2\pi nc^3\varepsilon_\infty m_t^2)\,[(K+2)/3K + (N_t/3N_v)]\,6N_v, \quad (20)$$

where the total carrier density is $N = 6N_v + 2N_t$, N_v is the carrier density in the valleys which are ascend, and $N_v + N_t$ is the carrier density in the valleys that descend, $\omega_l = Be/m_l$, $\omega_t = Be/m_t$, $k_\pm$ and $n_\pm$ are the extinction coefficients and the refractive indices of right- and left-handed polarized waves.

The ratio of the angle of rotation θ_s under a load to the angle of rotation θ_0 in the absence of a load is

$$\theta_{s(6)}/\theta_0 = [1 + KN_t/N_v(K+2)]\,[1 + (N_t/3N_v)]^{-1}. \quad (21)$$

Under the same boundary conditions the formula for a four-valley band is

$$\theta_{s(4)} = (e^3B\lambda^2 d/2\pi nc^3\varepsilon_\infty m_t^2)\,[(K+2)/3K + (N_t/4N_v)]\,4N_v,$$

where the total carrier density is $N = 4N_v + N_t$, N_v and N_t are the carrier densities in the ascending and descending valleys, respectively.

The ratio of the angles $\theta_{s(4)}$ and θ_0 is given by

$$\theta_{s(4)}/\theta_0 = \{1 + [3K/(K+2)]\,(N_t/4N_v)\}\,[1 + (N_t/4N_v)]^{-1}. \quad (22)$$

Under the Boltzmann statistics conditions the relative populations of the upper and lower valleys obey

$$(N_v + N_t)/N_v = \exp(\Delta E/kT),$$

where ΔE is the splitting of the valleys:

$$\Delta E_c[100] = c_{11}^{-1}\Xi_u T,\ \Delta E_f[100] = (c_{11} - c_{12})^{-1}\Xi_u T,$$
$$\Delta E_c[111] = (8/3)(c_{11} + 2c_{12} + 4c_{44})^{-1}\Xi_u T,\ \Delta E_f[111] = 4(9c_{44})^{-1}\Xi_u T; \quad (23)$$

here, c_{11}, c_{12}, and c_{44} are the elastic moduli of the crystal, Ξ_u is the deformation potential for pure shear, T is the average compressive stress, ΔE_c is the valley splitting on compression by radial stresses, ΔE_f is the valley splitting on compression of a free sample (no radial stresses). For germanium $\Delta E_c/\Delta E_f = 0.81$ and for silicon $\Delta E_c/\Delta E_f = 0.61$.

Figure 6 shows the dependences $\theta_{s(6)} = f_1(\Delta E/kT)$ and $\theta_{s(4)} = f_2(\Delta E/kT)$, calculated from Eqs. (20)–(22) for the directions [100] and [111] and K = 2, 3, and ∞. We can see that as the splitting ΔE increases in proportion to the load, in accordance with Eq. (23), the free-carrier rotation in a semiconductor with ellip-

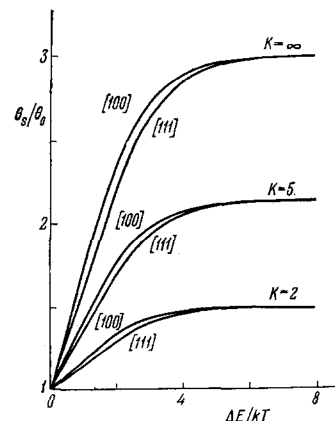

FIG. 6. Theoretical dependences of the angle of rotation on the splitting of equivalent valleys along the [100] and [111] directions for K = 2, 3, and ∞. [31]

soidal constant-energy surfaces increases and reaches saturation for $\Delta E/kT = 6$, where the saturation value θ_S/θ_0 depends much more strongly on K for low values of K than for large ones.

Measurements of the free-carrier rotation at various temperatures[32,33] make it possible to determine the temperature dependence of the effective mass more reliably than by other methods because the temperature dependences of all the quantities in Eq. (14) can be controlled quite easily.

Heating of carriers by a strong external electric field oriented in a suitable manner relative to the constant-energy ellipsoids results in a redistribution of carriers between the cold and hot valleys. This alters the angle of rotation of the plane of polarization[34-37] and such a change can be used to determine the band parameters. In semiconductors with spherical constant-energy surfaces the free-carrier rotation may decrease under the action of a strong electric field if the dispersion law is nonquadratic.[38]

III. EXPERIMENTAL RESULTS

5. Interband Effect

The oscillations in the spectra of the angle of rotation in the $\omega > \omega_g$ range can be resolved if the magnetic field, thickness of the sample, temperature, impurity concentration, and free-carrier density satisfy certain definite conditions. Since the lifetime of the Landau levels at any given temperature is not infinite, the level width is finite and the oscillations can be resolved if the magnetic field is sufficient to make the energy gap between the Landau levels greater than the level width, i.e., $\omega_{c,i}\tau_i \gg 1$, where $\omega_{c,i}$ and τ_i is the cyclotron frequency and the lifetime in the i-th band. For interband transitions this condition is of the form

$$\omega_* \tau_* \gg 1, \tag{24}$$

where $\omega_* = \omega_{c,n} + \omega_{c,p}$ and $\tau_* = \tau_c\tau_v(\tau_c + \tau_v)^{-1}$.

If we make allowance for the spin splitting, the condition of Eq. (24) for the resolution of the oscillations should be replaced by a more stringent requirement $kT \ll h\omega_s$.

Since the oscillatory interband effects are observed in the region of strong (fundamental) absorption of a crystal, the thickness of a sample d given by the minimum-error condition $\alpha d \approx 1$ is several microns and the sample should not be supported by a substrate if errors due to deformation are to be avoided. The condition (24) can be satisfied more easily for low impurity concentrations, low carrier densities, and low temperatures. Under these conditions the oscillations of the interband rotation become clearer in the $\omega > \omega_g$ range.

Oscillations of the angle of rotation in the nonresonance region $\omega < \omega_g$, which are due to the "blocking" of the interband transitions by free carriers in the Landau sub-bands of a degenerate semiconductor, can be observed if the temperature is low and the magnetic field is high so that the spin splitting $g\beta B$ exceeds the thermal energy of carriers, i.e., $g\beta B > kT$. Moreover, it is necessary to satisfy the condition $l\hbar\omega_c \approx E_F$, where the number of the Landau level l should not exceed 5—7 so that oscillations corresponding to the coincidence of the Fermi level and the 0! Landau level can be observed in reasonably strong magnetic fields.

The condition for sufficiently reliable determination of the effective mass of free carriers from the angle of rotation in the $\omega \ll \omega_g$ region, where this angle is inversely proportional to the square of the frequency, is given by the formula

$$\theta/\alpha d \approx \mu B/2,$$

where α is the absorption coefficient and μ is the free-carrier mobility. If we bear in mind that the measurement of the angle of rotation of 1° causes no special difficulties in the range of weak transmission, where $\alpha d \approx 4$ it follows that $\mu B \geq 10^{-2}$ whereas in the determination of the effective mass from cyclotron resonance one has to satisfy a much more stringent condition $\mu B \geq 1$, i.e., the Faraday effect can be used to determine the effective mass of carriers whose mobility is two orders of magnitude lower than those that can be studied under cyclotron resonance conditions.

A. Germanium. The interband rotation in this material has been investigated by many workers[26,39-43] at frequencies $\omega < \omega_g$ and $\omega > \omega_g$. An analysis of the experimental results in the $\omega < \omega_g$ region was made by Roth[15] allowing for the complex structure of the valence band and he found that $g_{eff} = -6.0$. It is interesting to note that the experimental points fit well the dependence $n\theta(1/\lambda^2)$ calculated for an elementary oscillator and they give the correct value of the free-electron mass ($1.04m_0$). The inversion of the rotation in the short-wavelength region has initially been attributed to the competition between direct and indirect transitions,[40] but subsequent calculations[21,25] have demonstrated that the direct transitions predominate. The influence of impurities, temperature, and electric fields on the interband rotation spectrum has been studied in[13,14,24,44-48].

The results of investigation carried out in the $\omega > \omega_g$ region in weak and strong magnetic fields are of special interest because the singularities in the spectra obtained for this region are related directly to the fine features of the band structure. Figure 4 shows the $\theta(\omega)$ spectra obtained by Mitchell and Wallis[41] at 300°K for a 5.72-μ thick germanium sample (on a glass substrate) subjected to a magnetic field of 86 kG. similar results were obtained by Nishina and Lax[43] for a sample ~4-μ thick in a field of 56.7 kG. Figure 4 includes also (dashed curve) the spectrum calculated for the same conditions by Suzuki and Hanamura.[25] The clearly manifested similarity of these spectra is evidence of a considerable contribution of excitons to the rotation bands. At low temperatures these spectra are even more complex[43] because of the deformation of the sample by the substrate. This deformation lifts the degeneracy in the valence band and shifts the Landau and exciton levels. A sample attached to a substrate is subject to residual stresses even at room temperature and these stresses are responsible for the long-wavelength maximum in the experimental dependence $\theta(\omega)$ plotted in Fig. 4.

An oscillatory rotation spectrum associated with the indirect interband transitions was reported by Halpern[49] for oriented samples which were not attached to substrates and in which the carrier density did not exceed 10^{13} cm^{-3}. The spectrum was recorded at 1.7°K in fields up to 103 kG. An analysis was made allowing for the contribution of indirect excitons.

B. Silicon. The interband Faraday effect in silicon

has been investigated only in the $\omega < \omega_g$ region.[50-53] In the latest investigation[53] the author used oriented single-crystal samples of intrinsic silicon. These samples were 90-24 μ thick and a study was made of the dispersion of the angle of rotation of the plane of polarization in the photon energy range 0.45–2.05 eV at room temperature in a magnetic field of 20 kG. A comparison of the experimental results with the theories[13-15,40] established that the main contribution to the rotation in this frequency range is made by direct allowed transitions of energy 3.07 eV according to the theory[40] and 2.80 eV according to the theory[13], whereas indirect transitions of energy 1.18 eV according to[40] and 1.16 according to[13] make no significant contribution to the angle of rotation.

C. III-V compounds. In the $\omega \gtrsim \omega_g$ range the small effective mass of electrons in indium antimonide makes it possible to observe bands in the rotation spectrum even if the magnetic field is weak. These bands were studied by Pidgeon and Brown.[54] In a strong magnetic field the spectrum had a complex structure, shown in Fig. 7 for 53.0 and 96.5 kG. The dependences plotted in this figure were obtained at ~20°K for samples 4.5 μ thick which were not bonded to substrates and in which the impurity concentration did not exceed 10^{14} cm^{-3}. A detailed theoretical analysis was not made in[54] but it was pointed out that the rotation was proportional to the difference between the contributions of the $\Delta M_J = +1$ and the $\Delta M_J = -1$ transitions to the dispersion. Therefore, resonance singularities appeared in the rotation spectrum near the same points as for combinations of the σ_+ and σ_- spectra, which were analyzed in detail in[54] and yielded all the principal parameters of the complex band structure of indium antimonide.

Oscillations of the interband rotation in gallium arsenide were studied carefully by Narita, Kobayashi, and Koike[55] at 77°K in fields of 80 kG. They used samples 5-μ thick with impurity concentrations not exceeding 10^{16} cm^{-3}. The exciton contribution was allowed for by introducing an energy shift of the bands and the band profiles and amplitudes were described with the aid of the relaxation time concept.

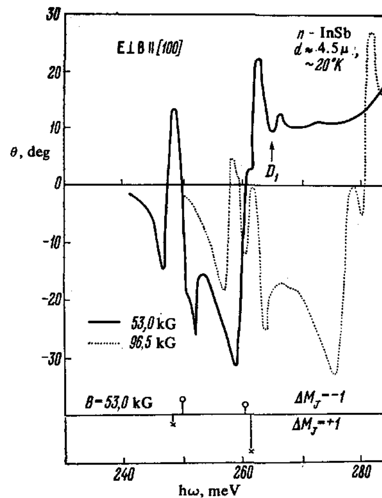

FIG. 7. Interband rotation spectra of n-type InSb at ~20°K in the $\omega \gtrsim \omega_g$ range. [54] The arrow identifies an induced transition D_1 whose intensity is 10 times lower than that of the allowed transition. The vertical lines at the bottom of the figure represent the intensities of the transitions with $\Delta M_J = -1$ and $\Delta M_J = +1$.

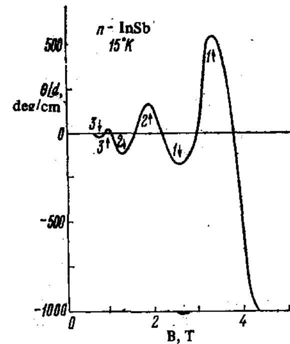

FIG. 8

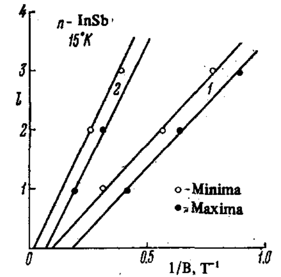

FIG. 9

FIG. 8. Oscillatory part of the dependence of the angle of rotation on the magnetic induction obtained for n-type InSb with an electron density of 5.0×10^{16} cm^{-3} at $\lambda = 6.2\mu$ and T = 15°K. [22]

FIG. 9. Experimentally obtained dependences [22] of the Landau numbers on the reciprocal of the magnetic induction, corresponding to minima and maxima in the oscillations of the angle of rotation, obtained for n-type InSb with electron densities of 5×10^{16} cm^{-3} (1) and 1.8×10^{17} cm^{-3} (2).

The first studies of the rotation in the $\omega < \omega_g$ range[42,50] were carried out at insufficiently low temperatures so that the influence of free carriers on the $\theta(\omega)$ spectrum was not determined correctly. Recently, Dennis, Smith, and Summers[22] studied the $\theta(\omega)$ spectrum of n-type InSb single crystals with electron densities from 10^{14} to 10^{17} cm^{-3}. The study was carried out at 15°K in magnetic fields up to 60 kG in the wavelength range 6–20 μ. Deviation of the dependence $\theta(B)$ from linearity was observed for a sample with an electron density of 1.5×10^{14} cm^{-3} and this deviation increased with decreasing wavelength in the range $\lambda > \lambda_g$, where $\lambda_g = \hbar 2\pi c/E_g$. In this case the Fermi energy was $E_F \sim 1$ meV and the thermal energy at 15°K was ~1.2 meV. Consequently, in magnetic fields B > 10 kG the spin-splitting energy $g\beta B$ exceeded considerably the Fermi energy E_F and the electrons populated only the sole Landau level (0↑). The degeneracy increased with the magnetic field intensity and this caused "blocking" of the lowest-energy allowed interband transition by free electrons and produced a positive contribution to the total angle of rotation.

Samples with electron densities of ~10^{17} cm^{-3} exhibited oscillations in the dependence of the angle of rotation on the magnetic induction in a wide range of the latter. The oscillations corresponded to crossing of the Fermi level by the Landau levels. Figure 8 shows only the oscillatory part of the dependence $\theta(B)$ for a sample with an electron density of 5.0×10^{16} cm^{-3} at $\lambda = 6.2$ μ. We can see that the amplitude of the oscillations decreases with increasing serial number of the Landau level and the larger amplitudes correspond to the spin-up Landau levels than to the spin-down levels, in agreement with the theory given in[20]. The positions of the extrema (Table II) are also in good agreement with the theory predicting values of the magnetic field corresponding to crossing of the Fermi level by the Landau levels (Fig. 3). The spectrum $\theta(B)$ has no oscillations corresponding to higher quantum numbers (lower magnetic fields) because in this case the quantization condition $g\beta B > kT$ is not obeyed so that electrons are redistributed between the neighboring Landau levels. Figure 9 shows the dependences $l(1/B)$ plotted in accordance with Eq. (9) for samples with electron

TABLE II. Comparison of theoretical and experimental values of magnetic induction corresponding to crossing of Fermi level by Landau levels

Electron density, cm^{-3}	Initial Landau level	Magnetic induction, T	
		Calc.	Expt.
$1.5\cdot10^{14}$	None	—	—
$8.0\cdot10^{15}$	0, −1/2	2.20	2.60
$5.0\cdot10^{16}$	0, −1/2	6.00	4.50
	1, +1/2	3.47	3.26
	1, −1/2	2.66	2.54
	2, +1/2	1.85	1.86
	2, −1/2	1.24	1.23
	3, +1/2	1.04	0.92
	3, −1/2	0.97	0.74
$1.0\cdot10^{17}$	1, −1/2	6.0	5.8
	2, +1/2	4.48	5.18
	2, −1/2	3.84	4.00
	3, +1/2	3.05	3.10
	3, −1/2	2.74	2.60

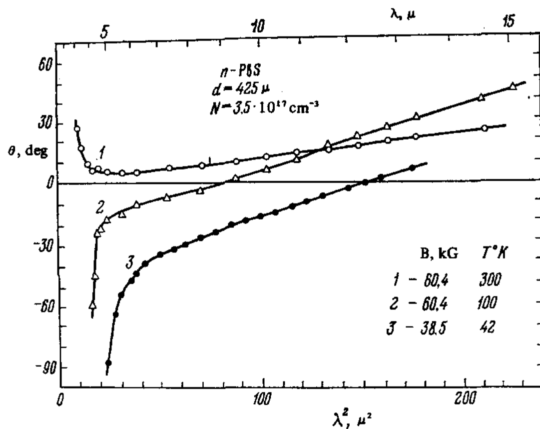

FIG. 10. Faraday effect spectra of PbS with an electron density of 3.5×10^{17} cm^{-3} at three different temperatures. [17]

densities of 5×10^{16} and 1.8×10^{17} cm^{-3}. The circular symbols in Fig. 9 represent the minima and maxima of the angle of rotation for magnetic inductions corresponding to the crossing of the Fermi level by the $(l, -1/2)$ and $(l, +1/2)$ Landau levels. The value of the g factor calculated by substituting the data of Fig. 8 into Eq. (9) is $-(47\pm1)$, in good agreement with the results of investigations carried out by other methods.

A considerable influence of impurities on the structure of the interband rotation in the $\omega < \omega_g$ region has been found for gallium antimonide and arsenide[19,58-62] but it has not yet been investigated in detail.

D. Lead chalcogenides. It was reported in[17,63] that the interband Faraday effect in n-type PbS exhibits two special features in the $\omega < \omega_g$ range: 1) the sign of the effect depends on temperature for a fixed electron density; 2) as $\omega \to 0$, the angle of rotation also decreases $\theta \to \theta_0 \neq 0$, where θ_0 is a function of temperature. Figure 10 shows the rotation spectra obtained at 300, 100, and 42°K for a sample 425-μ thick and with an electron density of 3.5×10^{17} cm^{-3}.[17] The inversion of the rotation in the temperature range 300—100°K can be seen quite clearly in Fig. 10. This can be explained, on the basis of Eq. (6), by the difference between the shift of the optical absorption edge (Burstein-Moss effect) for left- and right-handed polarized light. This difference depends strongly on the temperature of a crystal and on the electron density in an allowed band.

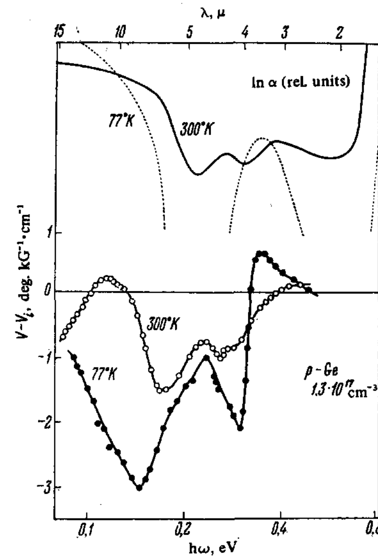

FIG. 11. Experimental Faraday effect spectra obtained at 300 and 77°K for p-type Ge with a hole density of 1.3×10^{17} cm^{-3}. The upper part of the figure shows the absorption spectra at 300 and 77°K. [10]

agreement with the experimental results. The interband rotation was also investigated in PbTe, PbSe,[29,64-66] and other semiconductors.[67-72] The influence of electric fields on the interband rotation was considered in[47,73].

6. Intraband Effect

The extinction coefficient governed by intraband transitions is small compared with the average value of the refractive index. Therefore, the Faraday effect, which is proportional to the difference between the refractive indices n_- and n_+ [Eq. (4)], is the only magnetooptic effect associated with these transitions that has been studied experimentally for p-type semiconductors.

A. Germanium. The intraband rotation spectra of p-type Ge were investigated by several workers.[10,28] The results of the most detailed investigation carried out by Lee and Fan[10] are plotted in Fig. 11 which shows the spectra due to the rotation associated solely with the transitions between the valence-band branches, i.e., the spectra in the lower part of Fig. 11 are the result of subtraction of the interband short-wavelength rotation from the experimental values. The upper part of Fig. 11 shows, for the sake of comparison, the absorption spectra of p-type Ge obtained at 300 and 77°K and plotted on a relative scale. We can clearly see a close analogy between the spectra, particularly at room temperature. The theory of the Faraday effect holds best at low temperatures and, therefore, the experimental results in Fig. 12 are compared with the theory only for 77°K. We can see that, apart from the long-wavelength part and the region near 0.3 eV the agreement between the theoretical and experimental spectra is quite satisfactory. The theoretical depth of the minimum near 0.3 eV can be reduced if it is assumed that the relaxation time is not the same for all the transitions but is shorter for the $V_3 \to V_1$ transition. According to Lee and Fan,[10] the long-wavelength maximum may be observed if measurements are extended to longer wavelengths.

The rotation associated with transitions within the

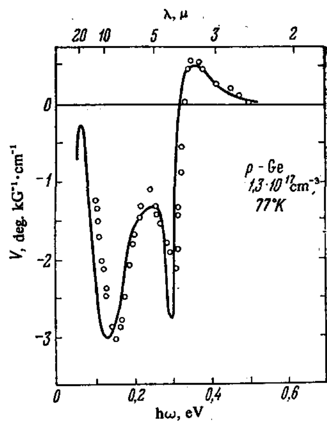

FIG. 12. Intraband rotation spectra of p-type Ge with a hole density of 1.3×10^{17} cm^{-3} at 77°K. The continuous curve is calculated and the points represent experimental values. [10]

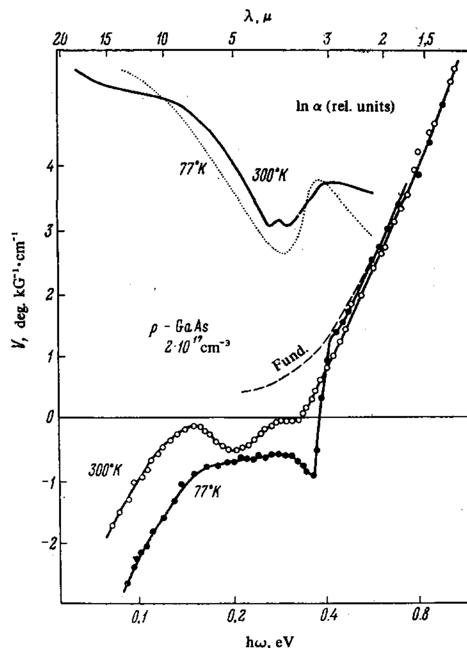

FIG. 13. Experimental spectra of the Faraday effect obtained at 300 and 77°K for p-type GaAs with a hole density of 2×10^{17} cm^{-3}. The upper part of the figure shows the absorption spectra at 300 and 77°K. [10]

The spectrum $n\theta(\omega)$ calculated from Eq. (6) is in good conduction and valence bands of silicon have not yet been definitely established.[52,72]

B. III-V compounds. It is not possible to detect the intraband rotation in p-type InSb because $\Delta_{so} > E_g$ and this rotation is masked by the much stronger interband rotation. In the case of GaAs, we have $\Delta_{so} < E_g$ and the effect should be observed clearly in the same way as in Ge.[10,28] Figure 13 shows the spectra obtained experimentally by Lee and Fan[10] at 77 and 300°K and, for the sake of comparison, the absorption spectra of p-type GaAs with a hole density of 2×10^{17} cm^{-3} (upper part of Fig. 13). The structures of the absorption and rotation spectra have much in common in the 3-15 μ range, which confirms that the mechanisms are the same but a detailed analysis of the spectra has not been made because some of the valence-band parameters of gallium arsenide must be refined. It has not yet been possible to isolate the intraband contribution to the total rotation in p-type InAs.[72]

C. IV-VI compounds. In contrast to germanium and gallium arsenide, the valence and conduction bands of PbS, PbSe, and PbTe are nondegenerate at the absolute extrema and, therefore, the intraband rotation does not occur in these compounds.[16,17,20,29,66]

7. Free-Carrier Effect

The free-carrier rotation of the plane of polarization provides a very convenient (from the practical point of view) method for the determination of the effective mass because if $\omega_g > \omega > \omega_p > \omega_{L0}$ the only limitation is the minimum angle of rotation. The sensitivity of the method can be raised by ensuring the optimal transparency of the sample selected so as to ensure maximum transparency but no interference. However, multiple reflection of light in a plane-parallel sample increases the measured angle of rotation θ_m.[74,75] If the angle of rotation is measured by crossing a polarizer with an analyzer (45° method), the relationship between θ_m and the angle θ in Eq. (14) is[10]

$$\theta \approx \theta_{изм}(1 + 2R^2 e^{-2\alpha d}\cos 4\theta_{изм}) \approx \theta_{изм}(1 - R^2 e^{-2\alpha d})/(1 + R^2 e^{-2\alpha d}).$$

If the absorption is weak ($e^{-2\alpha d} = 1$) and $\theta_m < 5°$, the measured angle θ_m exceeds the angle θ by 16.4%, which must be allowed for in the analysis of the experimental results.

A. Germanium. The free-electron rotation spectra are easier to investigate than the free-hole spectra because $m_n < m_p$; moreover, it is evident from Fig. 11 that the contribution of free holes cannot be separated easily from the intraband rotation in the $\omega < \omega_g$ range. The free-electron spectra $n\theta(\omega)$ in the frequency range from ω_g to ω_p are straight lines for samples with electron densities from 10^{16} to 10^{19} cm^{-3}. The slopes of these lines can be used, in accordance with Eq. (14), to determine the complex dependence of the Hall scattering factor on the electron density[76] on the assumption that the dispersion law near the L minimum is quadratic, i.e., that the mass is independent of the energy. Recently[77] a weak nonparabolicity of the L band has been revealed. Studies of the temperature dependence of $n\theta$ have established[32,33] that the effective electron mass m_n increases by 15% if the temperature is raised from 100 to 190°K.

B. Silicon. The effective mass of electrons in silicon is almost three times as large as in germanium and, therefore, it is more difficult to observe the free-electron rotation.[50-52] In a recent paper, Walton and Reimann[52] studied not only the dispersion of the rotation but also the dispersion of the refractive index up to λ = 25 μ for silicon samples with electron densities of 1×10^{18} and 4×10^{18} cm^{-3}. They determined the refractive index with high precision from the least-deflection angle in a prism. Simultaneous measurements of m_f and m_R should make it possible, in accordance with Eq. (18), to calculate the transverse component m_t of the effective mass, which was found to be $0.22m_0$ for the sample with the lower electron density and $0.23m_0$ for the sample with the higher density. Moreover, the mass was found to rise almost linearly with temperature, in agreement with the results of other workers.[32] The rise of the mass with temperature was somewhat more rapid than that expected from the change in the forbidden band width with temperature, but this can be attributed to a weak nonparabolicity of the conduction band of silicon. The nonparabolicity is also

supported by the observation that the transverse component of the effective mass m_t tends to rise with the degree of electron occupancy of this band.

The influence of uniaxial compression up to 5×10^9 dyn/cm^2 on the Faraday effect in n-type germanium and silicon samples doped to carrier densities of $\sim 10^{18}$ cm^{-3} was investigated by Dennis, Smith, and Summers[22] in the wavelength range $\lambda = 2-5\ \mu$ at room temperature in magnetic fields up to 33.9 kG. The splitting of the valleys in the conduction band ΔE was calculated from Eq. (23). Moreover, the same splitting was deduced experimentally from the splitting of the exciton lines in the absorption spectrum. In the $\lambda = 2-5\ \mu$ range the angle of rotation consisted of the interband $(D_1\lambda^{-2})$ and free-electron $(d_2\lambda^2)$ contributions, i.e., $\theta(\lambda) = D_1\lambda^{-2} + D_2\lambda^2$; therefore, the expresion

$$\theta\lambda^2 = D_1 + D_2\lambda^4$$

represents an equation of a straight line whose slope is proportional to the ratio of the density of free carriers to their effective mass.

Typical experimental dependences $\lambda^2\theta = f(\lambda^4)$ obtained for n-type Si under compression along the [$\bar{1}$00] axis are plotted in Fig. 14. The magnetic field and the direction of propagation of light were also oriented along the [100] axis. It is clear from Fig 14 that uniaxial compression increased the angle of rotation but did not affect its frequency dependence, in agreement with Eq. (20). We can see also that the intercept D_1 on the ordinate was not affected by compression, i.e., the interband rotation was independent of uniaxial compression up to 5×10^9 dyn/cm^2. This was due to the fact that the splitting of the equivalent valleys in the conduction band was small compared with the pressure-induced change in the forbidden band width.

Compression of n-type Ge along the [111] axis produced results similar to those plotted in Fig. 14 for n-type Si, but the angle of rotation was considerably larger because the effective mass of electrons in germanium is smaller than in silicon. However, in spite of the large angle of rotation, it was difficult to measure the ratio θ_S/θ_0 for n-type Ge because of strong birefringence resulting from uniaxial compression. The angle of rotation was not affected by compression of n-type Ge along the [100] axis because in this case all four ellipsoids of the conduction band were deformed in the same manner and the total electron density, their effective mass, and the refractive index of the crystal were not greatly affected.

The points in Fig. 15 represent the experimentally obtained dependences of the ratio θ_S/θ_0 on the splitting energy of valleys in the three samples of germanium. The continuous curves are the results of calculations

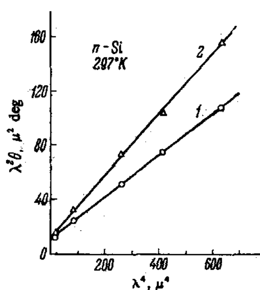

FIG. 14. Experimental dependences $\lambda^2\theta = f(\lambda^4)$ obtained [31] for n-type Si with an electron density of 7.6×10^{17} cm^{-3} on compression along the [100] axis (B = 33.9 kG). 1) No load; 2) $\approx 7 \times 10^9$ dyn/cm^2.

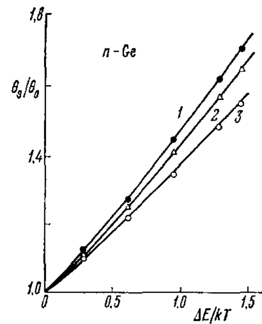

FIG. 15

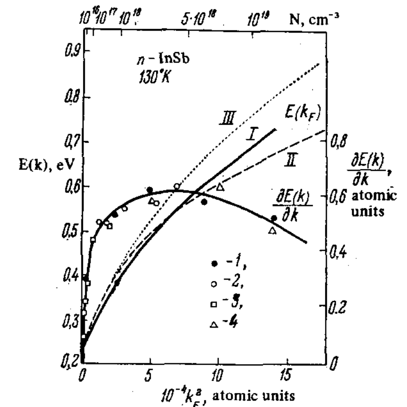

FIG. 16

FIG. 15. Dependences of the relative change in the angle of rotation on the energy of splitting of equivalent valleys in n-type Ge. [31] The continuous curves are theoretical: 1—$K = m_l/m_t = 17$, $N = 8 \times 10^{17}$ cm^{-3}; 2—$K = 11$, $N = 8 \times 10^{17}$ cm^{-3}; 3—$K = 7$, $N = 1.2 \times 10^{18}$ cm^{-3}.

FIG. 16. Dispersion relationships E(k) and $\partial E(k)/\partial k$ for the conduction band of InSb. [78] The experimental dependence is plotted to 130°K: $\partial E(k)/\partial k \propto k_F/m_n$. The values of masses m_n were deduced from the Faraday effect (1, 3) and from the refelction spectra (2, 4). I) $E(k_F)$; II), III) theoretical Kane dependences E(k) calculated without (II) and with (III) allowance for the contribution of upper bands.

based on Eq. (22) for a degenerate electron gas. Fitting of the calculated energy dependences of θ_S/θ_0 to the experimental results made it possible to determine the average values of $K = m_l/m_p$, which were 10^{+7}_{-3} for germanium and $4.3^{+0.6}_{-0.3}$ for silicon.

C. III-V compounds. The free-electron rotation in n-type InSb was found to be particularly strong in samples with low electron densities because the effective mass at the bottom of the conduction band was $m_{n0} = 0.013m_0$. Most of the investigations[78,8] of the free-electron Faraday effect have been concerned with the dispersion law E(k) of the conduction band of InSb because the dependence $m_n(N)$ for a nondegenerate band is related directly to E(k), in accordance with Eq. (15). Figure 16 shows the dispersion law E(k) deduced in[78] by graphical integration of the experimental dependence $m_n(N)$; the same figure includes the relations E(k) calculated on the basis of the Kane theory. We can see that at photon energies up to 0.6 eV the experimental dependence E(k) is in satisfactory agreement with the Kane curve which includes the contribution of the upper bands. It is also clear from Fig. 16 that m_f and m_R are equal. According to Eqs. (15), (16), and (19), this means that up to 10^{19} cm^{-3} all the electrons are concentrated in a single "spherical" band, i.e., the nearest higher conduction band lies at least 0.6 eV from the bottom of the absolute extremum.

In the case of n-type InAs with electron densities up to $N \approx 2 \times 10^{18}$ cm^{-3} it is found that $m_f = m_R$,[8,79-81] whereas in the range $N > 2 \times 10^{18}$ cm^{-3} the value of m_R exceeds m_f and the difference increases with the electron density.[82] It therefore follows from Eq. (16) that the conduction band must have a second branch separated by 0.2 eV and the effective mass in the second branch is $0.9m_0$.

An interesting feature of the free-electron rotation in n-type GaAs is the constant component $(\theta/d)_{\lambda=0} = \theta_0$, which increases with the electron density[83,84] in proportion to $N^{1/2}$, as shown in Fig. 17. This effect is

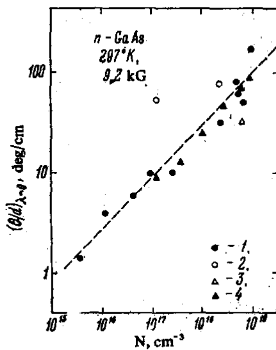

FIG. 17. Dependence of the zero intercept of the angle of rotation $(\theta/d)_{\lambda=0}$ on the electron density in n-type GaAs at 297°K. The dashed line represents $(\theta/d)_{\lambda=0} \propto N^{1/2}$. Experimental points: 1—taken from [83]; 2—[87]; 3—[59]; 4—[84].

attributed in[85] to multiple reflection and to inhomogeneities in the samples, but the results obtained by different workers[57,59,83,87] are in good agreement (Fig. 17). Multiple reflections have been allowed for in[59]. This allowance has not been made in[83] but such reflection cannot make a significant contribution in samples with electron densities in excess of 10^{18} cm^{-3}. However, the constant intercept may be due to different occupancies of the magnetic sub-bands.[16,17] A similar effect has been observed in n-type InSb.[22,88]

The temperature dependences $m_n(T)$ have been studied by the Faraday effect method for many III-V compounds[32,59] and it has been established that in the range 100—600°K the value of m_n at the Fermi level rises with temperature by 10—30% (depending on the compound).

The dependence of m_{pf} on the hole density in p-type GaAs was established in[28,89] from the free-hole rotation. Linear extrapolation yielded $m_{pf0} = 0.26m_0$ for zero hole density. Bearing in mind the relationship (17) between m_f and m_R and using the values of m_{f0} and $m_{R0} = 0.35m_0$, we calculated the masses of the heavy and light holes at the top of the valence band (m_{10} and m_{20}). At 300°K these masses were $m_{10} = 0.50m_0$ and $m_{20} = 0.80m_0$, which was in satisfactory agreement with the results of an analysis of the magnetooscillatory fundamental absorption spectra.[55] Knowing the values of m_{10} and m_{20} and the value $m_R = 0.44m_0$ for a hole density 1.2×10^{20} cm^{-3}, it was possible to use Eq. (16) in estimating the effective mass at the Fermi level. Its value, $m_2 = 0.4m_0$, was close to the heavy-hole mass, in qualitative agreement with the Kane theory (see[10]).

D. IV-VI compounds. The free-carrier rotation in these compounds has been investigated on many occassions[11,16,17,29,63,64,66,88] but most investigators have studied samples with a narrow range of carrier densities. These studies revealed temperature dependences of the effective masses in n- and p-type PbS and PbTe.[63,64] Since E_g for these compounds increases on heating, the rise of the effective mass is large compared with other semiconductors and it reaches 200% in the 100—300°K range. Figure 10 shows the rotation spectra[17] for one sample of n-type PbS at three different temperatures and the results show clearly the influence of the constant intercept θ_0 on the free-carrier rotation. Therefore, the effective mass can be determined from the slope of the linear dependence $n\theta(\lambda^2)$. The rotation spectra $n\theta(\lambda^2)$ have been determined[88] for p-type PbTe and PbSe films with hole densities from 10^{17} to 10^{20} cm^{-3} and a rapid rise of the mass with the carrier density has been observed, in agreement with the nonquadratic Kane dispersion law.

The free-carrier Faraday effect has been used in an analysis of the tensor of the reciprocal of the effective mass in silicon carbide,[90] tellurium,[91] and gallium antimonide,[92] in determination of the effective mass in various semiconductors,[93] and in a study of the carrier distribution across a crystal.[94] The influence of a strong ("heating") electric field on the free-electron rotation has been reported in[34-38,95].

IV. CONCLUSIONS

In the last decade the Faraday effect has been studied comprehensively in the interband transition range as well as at long infrared wavelengths. It has been used to determine the g factors of the energy bands and the gaps between special points in the Brillouin zone. Investigations of the free-carrier Faraday effect have proved to be most fruitful. The free-carrier rotation has been employed to determine accurately the effective masses of carriers and to find their dependences on the carrier density, which has made it possible to deduce the dispersion laws E(k) for energy bands in different semiconductors.

Recent theoretical investigations[35,38,47,73] have been concerned with the Faraday effect in crystals subjected simultaneously to a magnetic field and an electric field (perpendicular or parallel to the magnetic field), a stress field, or some combination of these fields. Further improvements in the experimental method, involving the use of lasers,[59,96] deep cooling, and strong magnetic and other fields, will undoubtedly reveal new features of the Faraday effect which can be used in studies of the band structures of semiconductors.

1. H. Kimmel, Z. Naturforsch. 12a, 1016 (1957).
2. B. Lax, Rev. Mod. Phys. 30, 122 (1958).
3. B. P. Zakharchenya and R. P. Seĭsyan, Usp. Fiz. Nauk 97, 193 (1969) [Sov. Phys.-Usp. 12, 70 (1969)].
4. E. Rashba, Usp. Fiz. Nauk 84, 557 (1964) [Sov. Phys.-Usp. 7, 833 (1965)].
5. T. S. Moss, Phys. Status Solidi 2, 601 (1962).
6. M. Rodot, Phys. Status Solidi 3, 1751 (1963).
7. M. Balkanski and E. Amzallag, Phys. Status Solidi 30, 407 (1968); E. Amzallag, Ann. Phys. (Paris) 5, 27 (1970).
8. Collection: Optical Properties of III-V Semiconductors (Russ. Transl.), Mir, M., 1970.
9. J. S. Blakemore, Semiconductor Statistics, Pergamon Press, Oxford, 1962 (Russ. Transl., Mir, M., 1964).
10. T. H. Lee and H. Y. Fan, Phys. Rev. 165, 927 (1968).
11. Yu. I. Ravich, B. A. Efimova, and I. A. Smirnov, Metody issledovaniya poluprovodnikov v primenenii k khal'kogenidam svintsa, Nauka, M., 1968 (Semiconducting Lead Chalcogenides, Plenum Press, New York, 1970).
12. L. I. Korovin, Fiz. Tverd. Tela 1, 1311 (1959); 3, 1790 (1961); 12, 945 (1970) [Sov. Phys.-Solid State 1, 1202 (1960); 3, 1299 (1961); 12, 739 (1970)].
13. I. M. Boswarva, R. E. Howard, and A. B. Lidiard, Proc. Roy. Soc. London A269, 125 (1962).
14. I. M. Boswarva and A. B. Lidiard, Proc. Roy. Soc. London A278, 588 (1964).
15. L. M. Roth, Phys. Rev. 133, A542 (1964).
16. E. D. Palik, D. L. Mitchell, and J. N. Zemel, Phys. Rev. 135, A763 (1964).
17. D. L. Mitchell, E. D. Palik, and R. F. Wallis, Phys. Rev. Lett., 14, 827 (1965).

[18]E. A. Stern, Phys. Rev. Lett. 15, 62 (1965).
[19]W. Thielemann and B. Rheinlander, Phys. Status Solidi 14, K205 (1966).
[20]D. L. Mitchell, E. D. Palik, and R. F. Wallis, Proc. Eight Intern. Conf. on Physics of Semiconductors, Kyoto, 1966, in: J. Phys. Soc. Jap. 21, Supplement, 197 (1966).
[21]P. S. Pershan, J. P. van der Ziel, and L. D. Malmstrom, Phys. Rev. 143, 574 (1966).
[22]R. B. Dennis, S. D. Smith, and C. J. Summers, Proc. Roy. Soc. London A321, 303 (1971).
[23]W. Thielemann, Phys. Status Solidi 26, K29 (1968).
[24]A. G. Zhilich and V. P. Makarov, Fiz. Tverd. Tela 6, 2058 (1964) [Sov. Phys.-Solid State 6, 1624 (1965)].
[25]K. Suzuki and E. Hanamura, J. Phys. Chem. Solids 30, 749 (1969).
[26]P. Byszewski and J. Dolodziejczak, Phys. Status Solidi 33, 485 (1969).
[27]J. Halpern, B. Lax, and Y. Nishina, Phys. Rev. 134, A140 (1964).
[28]A. K Walton and U. K. Mishra, Proc. Phys. Soc. London 90, 1111 (1967).
[29]S. Kurita, I. Nagasawa, K. Tanaka, Y. Nishina, and T. Fukuroi, Sci. Rep. Res. Inst. Tôhoku Univ. A17, 37 (1965).
[30]L. É. Gurevich and I. P. Ipatova, Zh. Eksp. Teor. Fiz. 37, 1324 (1959) [Sov. Phys.-JETP 10, 943 (1960)].
[31]A. K. Walton and C. R. Everett, Solid State Commun. 4, 211 (1966); A. K. Walton, P. L. Reimann, and C. R. Everett, J. Phys. C (Solid State Phys.) 4, 201 (1971).
[32]Yu. I. Ukhanov and Yu. V. Mal'tsev, Izv. Akad. Nauk SSR, Ser. Fiz. 28, 989 (1964).
[33]Yu. I. Ukhanov and Yu. V. Mal'tsev, Izv. Vyssh. Ucheb. Zaved., Fizika No. 5, 150 (1964).
[34]A. V. Subashiev, Fiz. Tverd. Tela 7, 936 (1965) [Sov. Phys.-Solid State 7, 751 (1965)].
[35]I. P. Ipatova, R. F. Kazarinov, and A. V. Subashiev, Fiz. Tverd. Tela, 7, 2129 (1965). [Sov. Phys.-Solid State 7, 1714 (1966)].
[36]D. Mukhopadhyay and B. R. Nag, Phys. Rev. B3, 360 (1971).
[37]H. Heinrich, Phys. Rev. B3, 416 (1971).
[38]L. E. Vorob'ev, V. I. Smirnov, U. B. Soltamov, V. I. Stafeev, and A. V. Shturbin, Fiz. Tekh. Poluprov. 1, 145 (1967) [Sov. Phys.-Semicond. 1, 114 (1967)].
[39]E. D. Palik, J. Phys. Chem. Solids 25, 767 (1964).
[40]J. Dolodziejczak, B. Lax, and Y. Nishina, Phys. Rev. 128, 2655 (1962).
[41]D. L. Mitchell and R. F. Wallis, Phys. Rev. 131, 1965 (1963).
[42]S. D. Smith, C. R. Pidgeon, and V. Prosser, Proc. Sixth Intern. Conf. on Physics of Semiconductors, Exeter, England, 1962, publ. by The Institute of Physics, London, 1962, p. 301.
[43]Y. Nishina, and B. Lax, J. Phys. Chem. Solids, 30, 739 (1969).
[44]M. I. Dyakonov, A. L. Efros, and D. L. Mitchell, Phys. Rev. 180, 819 (1969).
[45]E. G. Tsitsishvili, Fiz. Tekh. Poluprov. 4, 461 (1970) [Sov. Phys.-Semicond. 4, 386 (1970)].
[46]E. Haga, J. Phys. Soc. Jap. 20, 735 (1965).
[47]B. M. Askerov and F. M. Gashimzade, Fiz. Tverd. Tela 7, 3631 (1965) [Sov. Phys.-Solid State 7, 2926 (1966)].
[48]Ya. A. Rozneritsa and A. G. Chaban, Fiz. Tverd. Tela 8, 894 (1966) [Sov. Phys.-Solid State 8, 715 (1966)].
[49]J. Halpern, J. Phys. Chem. Solids 27, 1505 (1966).
[50]Yu. I. Ukhanov, Fiz. Tverd. Tela 4, 2741 (1962) [Sov. Phys.-Solid State 4, 2010 (1963)]; H. Piller and R. F. Potter, Phys. Rev. Lett., 9, 203 (1962).
[51]H. Stramska, Z. Bachan, P. Byszewski, and J. Kolodziejczak, Phys. Status Solidi 27, K25 (1968).
[52]A. K. Walton and P. L. Reimann, J. Phys. C (Solid State) 3, 1410 (1970).
[53]C. J. Gabriel, Phys. Rev. B2, 1812 (1970).
[54]C. R. Pidgeon and R. N. Brown, Phys. Rev. 146, 575 (1966).
[55]S. Narita, M. Kobayashi, and N. Koike, Proc. Ninth Intern. Conf. on Physics of Semiconductors, Moscow, 1968, Vol. 1, publ. by Nauka, Leningrad, 1968, p. 347.
[56]Z. I. Uritskiĭ and G. V. Shuster, Fiz. Tverd. Tela, 7, 3415 (1965) [Sov. Phys.-Solid State 7, 2752 (1966)].
[57]H. Piller, Proc. Eight Intern. Conf. on Physics of Semiconductors, Kyoto, 1966, in: J. Phys. Soc. Jap. 21, Supplement, 206 (1966).
[58]M. Zvara, Phys. Status Solidi 27, K157 (1968).
[59]H. Piller, see[55], p. 353.
[60]W. Thielemann, Phys. Status Solidi 34, 519 (1969).
[61]L. Ya. Baklaev, A. N. Levkov, and Yu. Ya. Umrilov, Fiz. Tekh. Poluprov., 4, 2015 (1970) [Sov. Phys.-Semicond. 4, 1730 (1971)].
[62]M. Zvara, Phys. Status Solidi 36, 785 (1969).
[63]Yu. V. Mal'tsev, E. D. Nensberg, A. V. Petrov, S. A. Semiletov, and Yu. I. Ukhanov, Fiz. Tverd. Tela 8, 2154 (1966). [Sov. Phys.-Solid State 8, 1713 (1967)].
[64]Yu. V. Maltsev, I. K. Smirnov, Yu. I. Ukhanov, and A. N. Veis, J. Phys. (Paris) 29, Suppl., C4-99 (1968).
[65]M. S. Kozyreva, Fiz. Tekh. Poluprov., 4, 1167 (1970) [Sov. Phys.-Semicond. 4, 986 (1970)].
[66]S. Kurita, J. Phys. Soc. Jap. 22, 1150 (1967).
[67]A. Ebina, T. Koda, and S. Shionoya, J. Phys. Chem. Solids 26, 1497 (1965).
[68]M. Balkanski, E. Amzallag, and D. Langer, Phys. Status Solidi 11, K59 (1965).
[69]Y. Nishina, S. Kurita, and S. Sugano, J. Phys. Soc. Jap. 21, 1609 (1966).
[70]M. Balkanski, E. Amzallag, and D. Langer, J. Phys. Chem. Solids 27, 299 (1966).
[71]M. Zvara, F. Žaloudek, and V. Prosser, Phys. Status Solidi 16, K21 (1966).
[72]U. K. Mishra and A. K. Walton, Phys. Status Solidi 24, K87 (1967).
[73]Q. H. F. Vrehen, W. Zawadzki, and M. Reine, Phys. Rev. 158, 702 (1967).
[74]E. D. Palik, J. R. Stevenson, and J. Webster, J. Appl. Phys. 37, 1982 (1966).
[75]V. D. Tron'ko, Opt. Spektrosk. 26, 484 (1969).
[76]A. K. Walton and T. S. Moss, Proc. Phys. Soc. London 78, 1393 (1961).
[77]R. L. Aggarwal, M. D. Zuteck, and B. Lax, Phys. Rev. 180, 800 (1969).
[78]F. P. Kesamanly, Yu. V. Mal'tsev, D. N. Nasledov, Yu. I. Ukhanov, and A. S. Filipchenko, Fiz. Tverd. Tela 8, 1176 (1966) [Sov. Phys.-Solid State 8, 938 (1966)].
[79]S. G. Shul'man and Yu. I. Ukhanov, Fiz. Tverd. Tela 7, 952 (1965) [Sov. Phys.-Solid State 7, 768 (1965)].
[80]C. J. Summers and S. D. Smith, Proc. Phys. Soc. London 92, 215 (1967).
[81]F. P. Kesamanly, Yu. V. Mal'tsev, D. N. Nasledov, L. A. Nikolaeva, M. N. Pivovarov, V. A. Skripkin, and Yu. I. Ukhanov, Fiz. Tekh. Poluprov. 3, 1182 (1969) [Sov. Phys.-Semicond. 3, 993 (1970)].
[82]L. A. Kazakova, V. V. Kostsova, R. K. Karymshakov, Yu. I. Ukhanov, and V. P. Yagup'ev, Fiz. Tekh. Poluprov. 5, 1710 (1971) [Sov. Phys.-Semicond. 5,

1495 (1972)].
[83]Yu. I. Ukhanov, Fiz. Tverd. Tela 5, 108 (1963) [Sov. Phys.-Solid State 5, 75 (1963)].
[84]P. B. Orlov, L. I. Kolesnik, and Yu. V. Kudin, Zavod. Lab. 37, 440 (1971).
[85]Yu. P. Mashukov, Fiz. Tekh. Poluprov. 1, 990 (1967) [Sov. Phys.-Semicond. 1, 828 (1968)]; A. V. Kravchenko and Yu. P. Mashukov, Izv. Vyssh. Ucheb. Zaved., Fizika No. 4, 100 (1971)
[86]H. Piller, Proc. Seventh Intern. Conf. on Physics of Semiconductors, Paris, 1964, Vol. 1, Physics of Semiconductors, publ. by Dunod, Paris; Academic Press, New York, 1964, p. 297.
[87]M. Cardona, Phys. Rev. 121, 752 (1961).
[88]M. S. Kozyreva and N. B. Arzheukhova, Fiz. Tekh. Poluprov. 4, 2172 (1970) [Sov. Phys.-Semicond. 4, 1862 (1971)].
[89]A. K. Walton and U. K. Mishra, J. Phys. C (Solid State) 1, 533 (1968).
[90]B. Ellis and T. S. Moss, Proc. Roy. Soc. London **A299**, 383 (1967).
[91]J. L. Callies and C. Rigaux, J. Phys. Chem. Solids 25, 1363 (1964).
[92]C. Y. Liang, H. Piller, and D. L. Stierwalt, Appl. Phys. Lett. 12, 49 (1968); G. Bordure and F. Guastavino, C. R. Acad. Sci. B267, 860 (1968).
[93]F. P. Kesamanly, É. É. Klotyn'sh, Yu. V. Mal'tsev, D. N. Nasledov, and Yu. I. Ukhanov, Fiz. Tverd. Tela 6, 134 (1964) [Sov. Phys.-Solid State 6, 108 (1964)]. J. Halpern, Rep. on Solid State Res. at Lincoln Lab., MIT, No. 2, 67, No. 3, 38, No. 4, 51, (1965); G. A. Sikharulidze, V. M. Tuchkevich, Yu. I. Ukhanov, and Yu. V. Shmartsev, Fiz. Tverd. Tela 8, 1159 (1966) [Sov. Phys.-Solid State 8, 924 (1966)]; S. Narita and A. Shibatani, J. Phys. Soc. Jap. 21, 1218 (1966); W. S. Baer, Phys. Rev. Lett. 16, 729 (1966); Phys. Rev. 154, 785 (1967); E. P. Andreeva, L. K. Diĭkov, M. S. Kozyreva, and N. N. Kolpakova, Izv. Sib. Otd. Akad. Nauk SSSR, Ser. Khim. Nauk No. 4(9), 5 (1967); V. K. Miloslavskiĭ, V. V. Karmazin, and A. A. Shapiro, Fiz. Tekh. Poluprov. 2, 590 (1968) [Sov. Phys.-Semicond. 2, 486 (1968)]; E. H. van Tongerloo and J. C. Woolley, Can. J. Phys. 46, 1199 (1968); K. K. Chandler and P. R. Wallace, Can. J. Phys. 47, 31 (1969); Yu. A. Makhalov and R. P. Melik-Davtyan, Fiz. Tverd. Tela 11, 2667 (1969) [Sov. Phys.-Solid State 11, 2155 (1970)]; V. V. Karmazin and V. K. Miloslavskiĭ, Opt. Spektrosk. 27, 78 (1969); V. V. Volkov, L. V. Volkova, and P. S. Kireev, Fiz. Tekh. Poluprov. 4, 1138 (1970) [Sov. Phys.-Semicond. 4, 961 (1970)]; Yu. M Burdukov, Yu. V. Mal'tsev, G. I. Pichakhchi, Yu. I. Ukhanov, and Kh. A. Khalilov, Fiz. Tekh. Poluprov. 4, 1390 (1970) [Sov. Phys.-Semicond. 4, 1184 (1971)]; Yu. M. Kozlov, G. I. Pichakhchi, V. G. Sidorov, and Yu. I. Ukhanov, Fiz. Tekh. Poluprov. 4, 1824 (1970) [Sov. Phys.-Semicond. 4, 1571 (1971)]; V. V. Karmazin and V. K. Miloslavskiĭ, Ukr. Fiz. Zh. 16, 547 (1971).
[94]R. R. Alfano and D. H. Baird, J. Appl. Phys. 39, 2931 (1968); M. H. Engiener, and B. R. Nag, J. Appl. Phys. 36, 3387 (1965).
[95]S. N. Baranovskiĭ and D. D. Bereznikov, Sbornik: Fizika i tekhnika poluprovodnikov (Collection: Physics and Technology of Semiconductors), NÉI, Novosibirsk, 1970.
[96]M. Shimura, N. Takeuchi, and T. Yajima, Jap. J. Appl. Phys. 9, 1334 (1970).

Translated by A. Tybulewicz